Bull. Chem. Soc. Ethiop. **2024**, 38(1), 229-239.
DOI: https://dx.doi.org/10.4314/bcse.v38i1.17

ISSN 1011-3924
Printed in Ethiopia
Online ISSN 1726-801X

SYNTHESIS, CRYSTAL STRUCTURE, DFT CALCULATION AND HIRSHFELD SURFACE ANALYSIS OF N-(4-METHYL PHENYL)-2-(3-NITRO-BENZAMIDO) BENZAMIDE

Mzgin Mohammed Ayoob* and Farouq Emam Hawaiz

Department of Chemistry, College of Education, Salahaddin University-Erbil, 44001, Erbil, Kurdistan, Iraq

(Received May 4, 2023; Revised September 6, 2023; Accepted September 18, 2023)

ABSTRACT. A new bis amide *N*-(4-methylphenyl)-2-(3-nitrobenzamide) benzamide was synthesized from a ring-opening reaction of 2-(3-nitrophenyl)-4*H*-benzoxazin-4-one, with 4-methyl aniline in a shorten reaction time (1.0 min) and characterized using different spectroscopic techniques (FT-IR, ^{1}H-NMR, ^{13}C-NMR) and single-crystal X-ray diffraction (XRD). In the crystal lattice, the molecules are linked by N–H···O and C–H···O hydrogen bonds. The Hirshfeld surface analysis mapped over shape index, curvedness indices, d_{norm} revealed strong H...H and H...O/O...H and intermolecular connections a key contributors to crystal packing structure. Density functional theory (DFT) calculations were applied with B3LYP/6-311G(d) level to provide theoretical data along with HOMO-LUMO electronic energy with the MEP map.

KEY WORDS: Benzamide, Crystal structure, DFT calculation, Hirshfeld surface

INTRODUCTION

The formation of amide linkages is one of the most significant transformations in organic chemistry [1]. Additionally, it can be found in many pharmaceuticals and other products with natural activity, including approximately 25% of commercially available drugs [2]. It serves as a primary linker in peptides and several polymers. Amides are a diverse category of bioactive components that are present in plants and thus are crucial including both their growth and defence against environmental triggers [3-5].

Amides are important functional groups in biochemical and pharmacological processes, and are widely used as building blocks for the synthesis of other compounds [6]. The ring opening reaction to form amides involves the cleavage of a cyclic structure, such as a lactam or a cyclic imide, and the formation of an amide bond between an amino group and a carbonyl group. The ring opening reaction to form amides is often carried out using a nucleophilic substitution reaction, in which a nucleophile attacks the carbonyl group of the cyclic compound, displacing the leaving group and forming the amide bond. This reaction can be catalyzed by a variety of catalysts, such as acids or bases. The ring-opening reaction of oxazin-4-one to benzamide is an important synthetic transformation in organic chemistry and has been used in the synthesis of a wide range of compounds, including pharmaceuticals, natural products, and synthetic materials [7].

In the previous studies, many researchers synthesized diamides from ring-opening benzoxazine-4-one derivatives by using trifluoroacetic acid–dichloromethane [8], *m*-chloro-peroxy benzoic acid [9], and glacial acetic acid [10].

In the current research, a new compound known as 2-(3-nitro benzamide)-N-(*p*-tolyl) benzamide was synthesized and analyzed its molecular structure utilizing FT-IR, ^{1}H-NMR, and ^{13}C-NMR spectroscopy. To explore the impact of hydrogen bonds on the molecular structure, the Hirshfeld surface analysis was employed.

*Corresponding author. E-mail: Mzgin.ayoob@su.edu.krd, Farouq.hawaiz@su.edu.krd

EXPERIMENTAL

Materials and methods

Chemicals of the analytical grade were purchased from several brands (Scharlau, Fluka, Riedel-de Haen). The IR spectrum was recorded using Infrared Affinity-1 (Shimadzu) spectrometers using KBr pellets in the range 4000-400 cm^{-1}. Single-crystal X-ray structure measurement was performed at 293 K using a B STOE IPDS2 (293 K) diffractometer with a radiation wavelength of (λ = 0.71073 Å). The structures were drawn using the ChemDraw version20. $CDCl_3$ was utilized as a solvent for the nuclear magnetic resonance experiments (^1H and ^{13}C-NMR spectra were recorded) (Bruker spectrometer 400 MHz). In ppm, chemical shifts are displayed. Scientific Stuart SMP3 melting point equipment was used to measure the melting point.

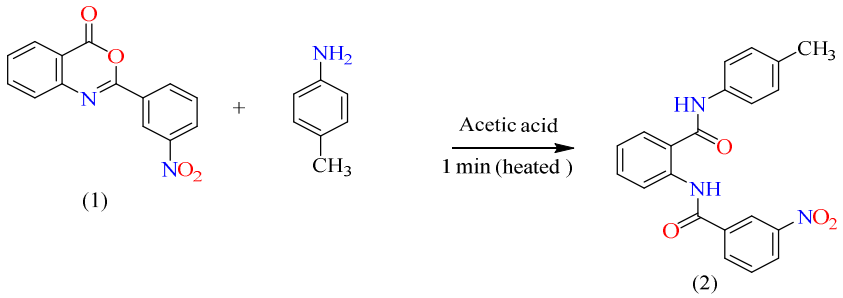

Scheme 1. The synthesis of bis amides.

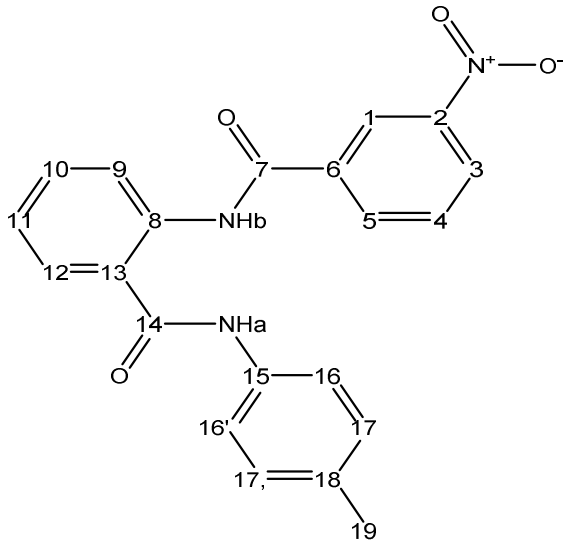

Figure 1. Numbered structure of bis amides.

Synthesis of 2-(3-nitrobenzamido)-N-(p-tolyl) benzamide

The synthesis of the titled compound as in (Scheme 1) was synthesized by the reaction of *p*-toluidine (321.21 mg, 3.00 mmol) with 2-(3-nitrophenyl)-4*H*-benzo-[1,3]oxazin-4-one (804.8 mg, 3.00 mmol) in glacial acetic acid (12 mL). It was heated, the solid product was collected within one minute [11]. The product was filtered out, and recrystallized from ethanol, to obtain a high-quality crystal, the bis amide was dissolved in acetic acid and let for 6 days to evaporate slowly to give the titled compound. $C_{21}H_{17}N_3O_4$: colorless crystal, yield: (89.3%), m.p. 191 °C. IR (KBr disc, cm^{-1}): 3311, 3093, 2983, 2924, 1685, 1631, 1616, 1527, 1352. ^{1}H-NMR (400 MHz, $CDCl_3$, δ, ppm): 2.44 (s, 3H, Ar-C$\underline{H}_3$), 7.15 (t,1H, C_{11}), 7.33 (d, 2H, $C_{17,17'}$), 7.4 6 (d,1H, C_{12}), 7.57 (t,1H, C_{10}), 7.64 (d,1H, $C_{16,16'}$), 7.71 (d,1H, C_5), 7.8 (t,1H, C_4), 8.36 (s,1H, C_1), 8.48 (d,1H, C_3), 8.73 (d,1H, C_9), 8.98 (s,1H, NHa), 12.2 (s,1H, HNb). ^{13}C-NMR (100 MHz, $CDCl_3$, δ, ppm): 167.45: C_{14} (C=O), 163.37: C_7, 148.75: C_2, 139.75: C_8, 136.62: C_6, 135.32: C_{18}, 134.65: C_{15}, 133.00: C_5, 132.7: C_{10}, 130.09: C_4, 129.87: $C_{17,17'}$, 126.96: C_{12}, 126.43:C_3, 123.65: C_{11}, 123.2: C_1, 122.01: C_{13}, 121.09: C_9, 121.07: $C_{16,16'}$, 21.05: Ar-$\underline{C}H_3$ (Figure 1).

X-Ray diffraction study

An appropriate colourless prism single-crystal was selected to collect X-ray diffraction data of $C_{21}H_{17}N_3O_4$ collected with graphite-monochromatized Mo-Kα radiation (λ = 0.71073 Å) on an STOE IPDS2 (293 K) diffractometer [12]. The structure of the compound was solved using SHELXT [13], and refinement was made with SHELXL-2018 with least-squares minimization versus *F*2 [14]. All the non-hydrogen atoms were refined with anisotropic displacement parameters. H atoms were placed in geometrically idealized positions and constrained to ride on their parent atoms with C—H distances in the range of 0.93–0.96 Å. (Table 1) summarized the experimental details for $C_{21}H_{17}N_3O_4$.

Table 1. X-Ray crystallographic data and structure refinements for $C_{21}H_{17}N_3O_4$.

Empirical formula	$C_{21}H_{17}N_3O_4$
Formula weight	375.38
Temperature/K	293
Crystal system	Monoclinic
Space group	$P2_1/c$
a/Å	13.4700(8)
b/Å	19.9078(16)
c/Å	13.8940(8)
α/°	90
β/°	95.174(5)
γ/°	90
Volume/Å3	3710.6(4)
Z	8
ρcalcg/cm3	1.344
μ/mm-1	0.095
F(000)	1568.0
Radiation	MoKα (λ = 0.71073)
Ø range for data collection/°	3.036 to 52
Index ranges	$-16 \le h \le 16$, $-24 \le k \le 24$, $-17 \le l \le 16$
Reflections collected	26350
Independent reflections	7290 [R_{int} = 0.0769, R_{sigma} = 0.0632]
Data/restraints/parameters	7290/0/523
Goodness-of-fit on F2	1.052
CCDC	2245098

Hirshfeld surface analysis

An input file for Hirshfeld surface visualization of the chemical was a crystallographic information file (CIF) generated from single-crystal X-ray diffraction to investigate the different interactions in the crystal structure of $C_{21}H_{17}N_3O_4$ compound, Hirshfeld surface analysis and Hirshfeld surface visualization[15], presentation of results fingerprint plots with dean de and di distances were generated from the crystal data were performed with the *CrystalExplorer21* program [16].

Computational study

An in-depth theoretical investigation of the molecular interactions was carried out to more accurately interpret the spectrum designations and analyze the molecular geometry and electronic transitions of the synthesized compound (**2**). For theoretical studies, the Gaussian 06.0.16 software was applied. The basis set B3LYP/6-311G(d) of Pople was used to perform gradient-adjusted correlation. The B3LYP/6-311G(d) basis set was also used to obtain optimized 2 structures. Highest occupied molecular orbital (HOMO), molecular electrostatic potential (MEP) map and lowest unoccupied molecular orbital (LUMO) were assessed. Additionally, this theory was used to compute structure-based molecular characteristics such as total energy, electron affinity, ionization energy, frontier molecular orbitals, molecular electrostatic potential and chemical softness [17].

RESULTS AND DISCUSSION

The amide 2-(3-nitrobenzamido)-*N*-(*p*-tolyl) benzamide was formed from ring opening reaction of 2-(3-nitrophenyl)-4H-benzo[1,3]oxazin-4-one with 4-methyl aniline. The structure of newly synthesized compounds was investigated by FT-IR, ^{1}H-NMR and ^{13}C-NMR. The presence of a band at 3311 cm^{-1} due to the ν (N-H stretching vibration of amide, furthermore, the appearance band at 1685 cm^{-1} due to the (C=O) stretching vibration of amide [18]. The appearance of bands at 1527 and 1352 cm^{-1} was due to the presence of the nitro group.

In ^{1}H-NMR, the appearance of a singlet signal at 2.44 ppm with three protons due to the methyl protons attached to the para position of aromatic moieties, the occurrence of two singlet signals at 8.98 and 12.2 ppm ascribed to the two amide (N-H) groups. In ^{13}C-NMR, the two-carbonyl group of amides appeared at 163.31 and 167.48 ppm for C_7 and C_{14} (C=O), respectively, and the methyl group appeared at 19.65 ppm.

The ORTEP representation of the $C_{21}H_{17}N_3O_4$ compound with atomic number is given in Figure 2. The displacement ellipsoids of the atoms other than the H atoms of the molecule are drawn with a 30% probability. The molecule of the title compound comprises a 3-nitro benzamide unit, 4-methyl aniline moiety and phenyl ring. The nitrobenzene substituent makes dihedral angles of 10.69 and 15.3° with the C13–C12 and C18–C19 rings, respectively. The C13–C12 ring is oriented at a 6.4° dihedral angle concerning 4-methyl aniline moiety. The amide groups C6/C7(O3)/N2/C13and C15/N3/C14(O4)/C12 which link the rings are inclined to C13–C12 ring by 16.32 and 44.86°, respectively. The nitro group forms a 12.09° angle with a ring of C5–C6, while the methyl group is approximately coplanar with a ring of C17–C18 ring, forming an angle of 0.76 °.

The bond lengths of the nitro groups, N1=O1 and N1=O2, in the structure, were determined as 1.228(5) and 1.215(4) Å. However, the bond lengths for the carbonyl groups, C7=O3 and C14=O4 were determined as 1.236 (4) and 1.236 (4) respectively. These C=O bond lengths are comparable to the values of 1.230 (4) and 1.2257 (17) Å previously reported by Simsek *et al* [19] and Mague [20]. In a work by Yu and Fu [21], N3=O8 [1.201 (7) Å] and N3=O9 [1.215 (6) Å] bond lengths are quite close to N3=O3 [1.219 (5) Å] and N3=O4 [1.218 (4) Å] bond distances in the title compound. The values of those bond lengths correspond to 1.235 (5) and 1.216 (5) Å in

previous work are slightly longer distances [22]. Also, compared to the C=O bond lengths in these works, the selected are consistent with the bond lengths in the title crystal. In the structure, the C–N bond lengths are typical of a single bond. The selected bond length values of the compound are given in Table 2.

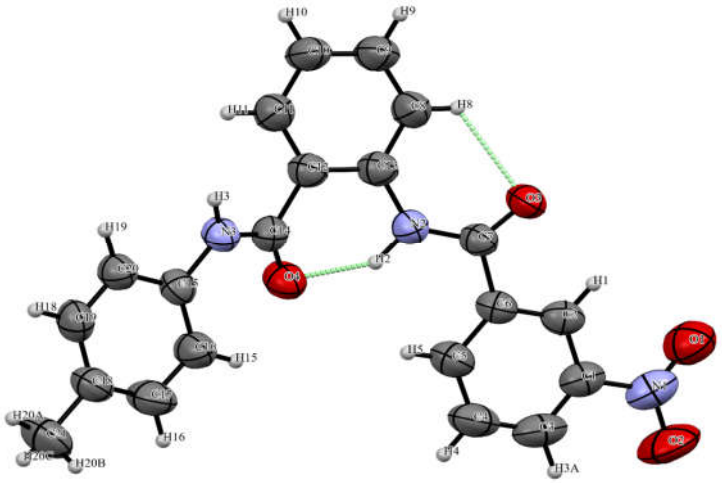

Figure 2. Crystal structure of formula molecule $C_{21}H_{17}N_3O_4$. ellipsoids with a 30% of probability.

In the crystal, the molecules are linked by C8–H8···O3, C15–H16···O4 and N2–H2···O4 intra-hydrogen bonds (Figure 3, Table 3) [22] generating two-dimensional layers propagating along the *a*-axis direction. The hydrogen atom of the 4-toluidine moiety is involved in the N3–H3···O3 hydrogen bond with the O3 atom of the benzamide substituent of adjacent molecules. The hydrogen atom of the C12–C13 benzene ring forms a C8–H8···O3 hydrogen bond with the carbonyl O3 atom of another adjacent molecule.

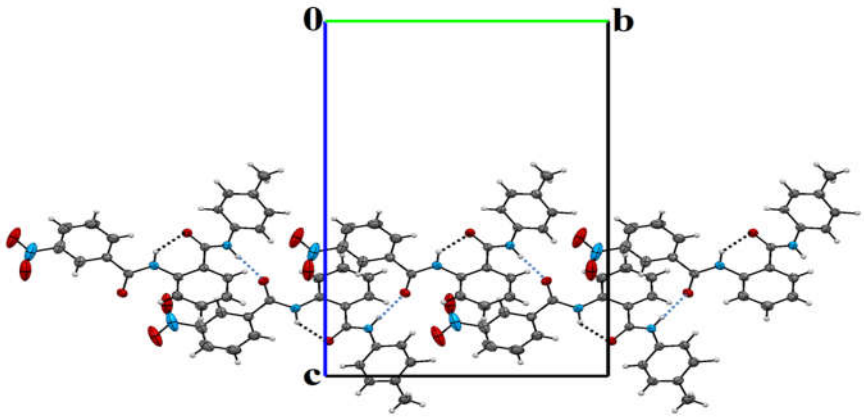

Figure 3. The packing of $C_{21}H_{17}N_3O_4$, showing the two-dimensional layers formed by N–H···O hydrogen bonds (dashed lines).

Table 2. Selected bond lengths of $C_{21}H_{17}N_3O_4$.

Bond length	Distance, Å	Bond length	Distance, Å
O3-C7	1.236(4)	C6-C5	1.394(5)
O4-C14	1.234(4)	C14-C12	1.521(5)
N3-C15	1.437(4)	C12-C11	1.391(5)
N3-C14	1.349(5)	C2-C1	1.374(5)
N2-C7	1.344(5)	C20-C19	1.398(5)
N2-C13	1.406(5)	C1-C3	1.356(6)
O1-N1	1.228(5)	C18-C19	1.368(5)
N1-C1	1.468(6)	C18-C17	1.372(6)
N1-O2	1.215(4)	C18-C21	1.525(5)
C15-C20	1.375(5)	C11-C10	1.387(5)
C15-C16	1.378(5)	C8-C9	1.376(5)
C7-C6	1.506(5)	C5-C4	1.381(6)
C13-C12	1.411(5)	C16-C17	1.394(5)
C13-C8	1.392(5)	C3-C4	1.379(6)
C6-C2	1.391(5)	C10-C9	1.370(6)

Table 3. Parameters of hydrogen bond in $C_{21}H_{17}N_3O_4$.

D–H···A	*d*(*D*–H)	*d*(H···A)	*d*(*D*···A)	*D*–H···A
C8–H8···O3	0.93	2.36	2.914 (5)	118.0
C15–H16···O4	0.93	2.39	2.931 (5)	116.6
N2–H2···O4	1.02	1.82 (5)	2.668(4)	139(4)

Hirshfeld surface analysis

A Hirshfeld surface analysis [23] and the associated two-dimensional fingerprint plots were generated using CrystalExplorer21 [24], with a standard resolution of the three-dimensional d_{norm} surfaces plotted over a fixed colour scale of -0.4781 (red) to 1.4321 (blue) a.u. while curvedness and shape index are mapped over the ranges – 4.0000 to 0.4000 Å and 1.0000 to 1.0000 Å, respectively. (Figure 4). Hirshfeld surface analysis is a method that examines intermolecular interactions[25]. These surfaces are used to visualize Van der Waals distances and to determine interaction points between molecules[26]. Hirshfeld surface maps include d_{norm}, d_i, d_e, as in Figure 4 (a-c) including shape index, de and curvedness indices, and the most basic surface map can be visualized with d_{norm}. the π···π stacking interaction was studied by curvedness and shape index, where red triangles indicate concave regions above the surface caused by the stacked compound's phenyl carbon atoms and blue triangles represent convex sections of the compound inside the surface [27], In Figure 4(c), The green planes seen on the benzene rings on the curvedness surface indicate closer regions on the surface and correspond to π···π interactions. The two-dimensional plot shows the main intermolecular interactions in the titled compound, H···H, H…O/O…H, C…H/H…C, C…C, C…O/O…C, C…N/N…C, H…N/N…H, and O…O, the maximum involvement to the complete Hirshfeld surface occurs due to H… H close contacts with 40 %. The percentages of H…O/O…H, C…H/H…C, C…C, C…O/O…C, C…N/N…C, H…N/N…H, and O…O interactions are 26.9, 13.8, 7.1, 6.6, 3.9, 1.6 and 0.1% of bis amide surface, respectively, and the two-dimensional fingerprint maps shown in Figure 5.

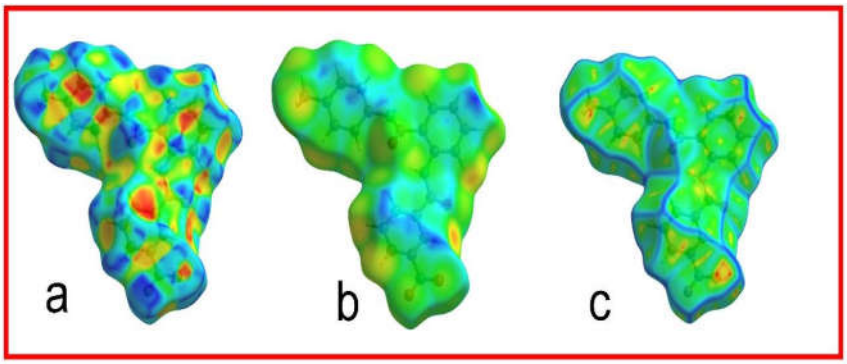

Figure 4. Hirshfeld surfaces of $C_{21}H_{17}N_3O_4$ with a) shape index, b) de, and c) curvedness.

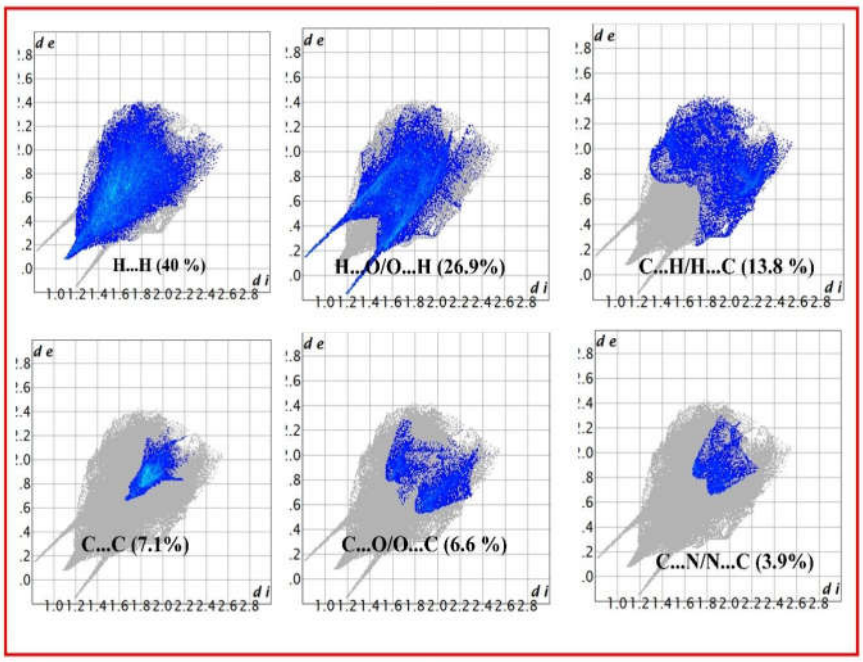

Figure 5. The view of the 2D fingerprint plots in $C_{21}H_{17}N_3O_4$.

DFT study

Computational study was utilized to look at the chemical interactions in greater depth, furthermore to research the synthetic substances' electrical transitions and molecular structure. The computational investigation was performed by utilizing the Gaussian 06.0.16 software. With Pople's basis set B3LYP/6-311G(d), the gradient-adjusted correlation was used [28]. Using the B3LYP/6-311G(d) basis set, optimized structures of 2 were also produced. A gradient-adjusted

correlation was applied using Pople's basis set B3LYP/6-311G(d). Moreover, bis-amide-optimized structures were generated. HOMO and LUMO play key roles in electronic studies [29], when a molecule's energy gap is less, it is seen as being softer and having better chemical reactivity. A molecule's stability is presumed to be good and its chemical hardness is considered to be higher when it has a high energy gap [30, 31].

Calculations were made for the energy occupied by the highest occupied molecular orbital (E-HOMO), lowest unoccupied molecular orbital (E-LUMO) and Molecular electrostatic potential (MEP) map [32], the (EHOMO, ELUMO), energy difference (ΔE) band gap energy, MEP and Mulliken charge are illustrated in Figure 6. The overall electronic energy value of a synthesized bis amide is -34694.5 eV. The dipole moment is 10.4 Debye, E-HOMO), (E-LUMO) and (ΔE) is -6.2254, -2.85093 and 3.37447 eV respectively, Negative values of E-HOMO) and (E-LUMO) it showed that the bis amide is thermodynamically stable [33, 34], the HOMO orbitals are distributed over the amide group and toluidine moieties and LUMO orbitals are mainly distributed over *meta*-nitro phenyl moieties. In the MEP map the red area represents the electronegative region and the blue area represents the electropositive region C, and H lies in the blue region, where O and N lie in the red region [35]. MEP map of bis amide is designed from deep red to deep blue colour scale from -6.916 e^2 to 6.916 e^2 it illustrates that the molecule has both preferred sites for nucleophile and electrophile attach [36, 37]. Finally, the results obtained from the Mulliken charge scaled from (-0.818 to 0.052) reveal a change in Mulliken charge which indicates the compound has a different structure value [38, 39].

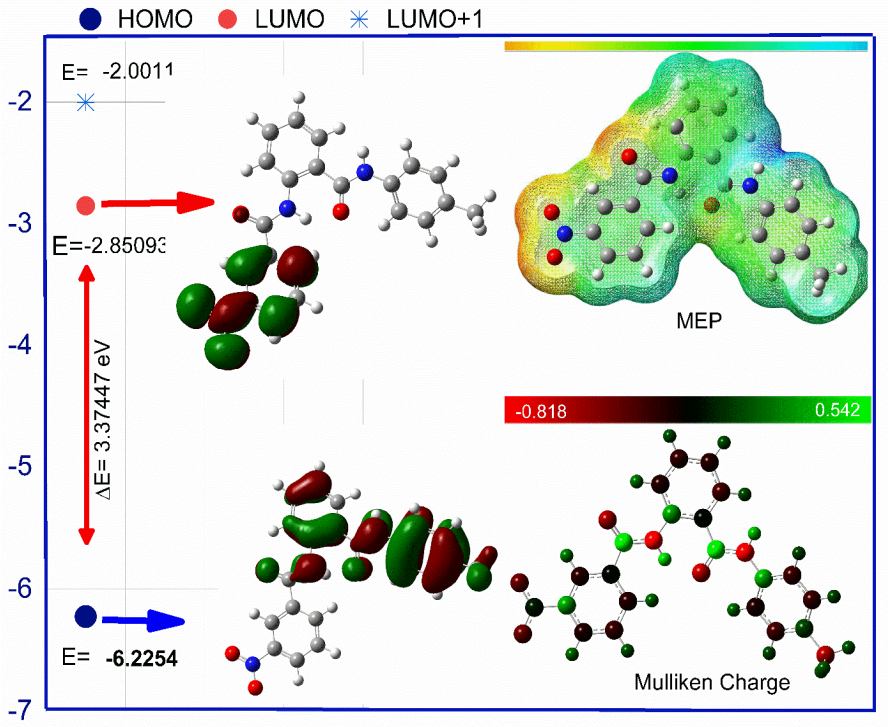

Figure 6. The diagram shows HOMO, LUMO and LUMO+1 with their band gap energies, MEP and Mulliken.

CONCLUSION

In this study, the compound *N*-(4-methyl phenyl)-2-(3-nitro-benzamide) benzamide was investigated by single-crystal XRD. In addition, IR, ^{1}H NMR, and ^{13}C NMR spectroscopic methods were used for structural characterization. The obtained results showed that it was compatible with the X-ray structure parameters. Hirshfeld surface analysis confirms that H···H, and H…O/O…H interactions are mainly responsible for the crystal packing of the compound. 2D fingerprint plots show that the largest contributions to the total Hirshfeld surface are due to the percentage of H…O/O…H, C…H/H…C, C…C, C…O/O…C, C…N/N…C, H…N/N…H, and O…O interactions are 26.9, 13.8, 7.1, 6.6, 3.9, 1.6 and 0.1%. Density functional theory (DFT) calculations were applied with basis sit B3LYP/6-311G(d) level of theory to provide theoretical data along with HOMO-LUMO electronic energy with MEP map.

ACKNOWLEDGMENTS

The authors would like to acknowledge the Department of Chemistry, College of Education, Salahaddin University-Erbil, Iraq for providing the facility to complete this study. We acknowledge Ondokuz Mayıs University for single-crystal X-ray diffraction analysis.

SUPPLEMENTARY MATERIALS

Crystallographic data for the bis amide have been deposited with the Cambridge Crystallographic Data Center (CCDC), with the deposit number 2245098. The data can be obtained free of charge via DOI: 10.5517/ccdc.csd.cc2fc6jk

REFERENCES

1. Greenberg, A.; Breneman, C.M.; Liebman, J.F. *The Amide Linkage: Structural Significance in Chemistry, Biochemistry, and Materials Science*, John Wiley and Sons: Toronto: Canada; **2000**; p 676.
2. Yaman, M.; Dege, N.; Ayoob, M.M.; Hussein, A.J.; Samad, M.K.; Fritsky, I.O. Hirshfeld surface analysis and crystal structure of N-(2-methoxyphenyl) acetamide. *Acta Cryst. E* **2019**, 75, 830-833.
3. Košak, U.; Gobec, S. A simple and effective synthesis of 3-and 4-((phenylcarbamoyl) oxy) benzoic acids. *Acta Chim. Slov.* **2020**, 67, 940-948.
4. Kovač, N.; Faganeli, J.; Bajt, O.; Šket, B.; Vuk, A.Š.; Orel, B.; Mozetič, P. Degradation and preservation of organic matter in marine macroaggregates. *Acta Chim. Slov.* **2006**, 53, 81-87.
5. Pattabiraman, V.R.; Bode, J.W. Rethinking amide bond synthesis. *Nature* **2011**, 480, 471-479.
6. Ghoshal, T. Electrochemical synthesis of 4-quinazolinone derivatives mediated by acetic acid. *ARK.* **2023**, 13, S1-S33.
7. Ramadan, S.K.; Abou-Elmagd, W.S.; Hashem, A.I. Reactions of 2(3H)-furanones. *Synth. Commun.* **2019**, 49, 3031-3057.
8. Kulangiappar, K.; Anbukulandainathan, M.; Raju, T. Nuclear versus side-chain bromination of 4-methoxy toluene by an electrochemical method. *Synth. Commun.* 2014, 44, 2494-2502.
9. Rajesh, N.; Manisha, B.; Ranjith, J.; Krishna, P.R., A metal-free tandem ring-opening/ring-closing strategy for the heterocyclic conversion of benzoxazin-4-ones to oxazolines. *RSC Adv.* **2016**, 6, 6058-6064.

10. Ayoob, M.; Hawaiz, F.; Dege, N.; Kansız, S. Structural investigation and Hirshfeld surface analysis of N-(3-chloro-4-methylphenyl)-2-(3-nitrobenzamido) benzamide. *J. Struct. Chem.* **2023**, 64, 1049-1058.
11. Ayoob, M.M.; Hawaiz, F.E. Design, synthesis, molecular docking ADMET and anti-bacterial activities of some new benzamides and their corresponding quinazolinone derivatives. *Egypt. J. Chem.* **2022**, 65, 1517-1530.
12. Stoe, C. *X-area (version 1.18) and X-red32 (version 1.04)*, Stoe & Cie: Darmstadt, Germany; **2002**.
13. Sheldrick, G.M. SHELXT–integrated space-group and crystal-structure determination. *Acta Crystallogr. A Found Adv.* **2015**, 71, 3-8.
14. Sheldrick, G.M. Crystal structure refinement with SHELXL. *Acta Crystallogr. C Struct. Chem.* **2015**, 71, 3-8.
15. Rafik, A.; Zouihri, H.; Guedira, T. Hirshfeld surface analysis and quantum chemical study of molecular structure of phosphate. *Bull. Chem. Soc. Ethiop.* **2021**, 35, 625-638.
16. Van Thong, P.; Chi, N.T.T.; Azam, M.; Hanh, C.H.; Alam, M.; Al-Resayes, S.I.; Van Hai, N. NMR investigations on a series of diplatinum(II) complexes possessing phenylpropenoids in $CDCl_3$ and CD_3CN: Crystal structure of a mononuclear platinum complex. *Polyhed.* **2022**, 212, 115612.
17. Kınaytürk, N.K.; Önem, E.; Oturak, H. Benzoic acid derivatives: Anti-biofilm activity in *Pseudomonas aeruginosa* PAO1, quantum chemical calculations by DFT and molecular docking study. *Bull. Chem. Soc. Ethiop.* **2023**, 37, 171-181.
18. Moreno-Fuquen, R.; Arango-Daraviña, K.; Becerra, D.; Castillo, J.-C.; Kennedy, A.R.; Macías, M.A. Catalyst-and solvent-free synthesis of 2-fluoro-N-(3-methylsulfanyl-1H-1,2,4-triazol-5-yl) benzamide through a microwave-assisted Fries rearrangement: X-ray structural and theoretical studies. *Acta Crystallogr. C Struct. Chem.* **2019**, 75, 359-371.
19. Simsek, O.; Dincer, M.; Dege, N.; Saif, E.; Yilmaz, I.; Cukurovali, A. Crystal structure and Hirshfeld surface analysis of (Z)-4-{[4-(3-methyl-3-phenylcyclobutyl) thiazol-2-yl] amino}-4-oxobut-2-enoic acid. *Acta Cryst. E* **2022**, 78, 120-124.
20. Mague, J.; Mohamed, S.; Akkurt, M.; Bakhite, E.; Albayati, M. 2-({5-[(4-Chlorophenoxy) methyl]-4-phenyl-4H-1,2,4-triazol-3-yl}sulfanyl)-N-phenylacetamide. *IUCrData* **2016**, 1, x160453.
21. Yu, C.-Y.;Fu, Y. 1,4-Dideoxy-2,3-O-isopropylidene-N-[3-(3-nitrobenzoylamino)benzoyl]-1, 4-imino-d-talitol. *Acta Crystallogr. Sect E Struct. Rep. Online* **2006**, 62, o3113-o3114.
22. Moreno-Fuquen, R.; Hurtado-Angulo, M.; Arango-Daravina, K.; Bain, G.; Kennedy, A.R. Synthesis, crystal structure, Hirshfeld surface analysis, MEP study and molecular docking of N-{3-[(4-methoxyphenyl) carbamoyl] phenyl}-3-nitrobenzamide as a promising inhibitor of hfXa. *Acta Cryst. E* **2020**, 76, 1762-1767.
23. Spackman, M.A.; Jayatilaka, D. Hirshfeld surface analysis. *CrystEngComm* 2009, 11, 19-32.
24. Wolff, S.; Grimwood, D.; McKinnon, J.; Turner, M.; Jayatilaka, D.; Spackman, M. *Crystal Explorer*. University of Western Australia Crawley, Australia, **2012**.
25. Ashfaq, M.; Munawar, K.S.; Tahir, M.N.; Dege, N.; Yaman, M.; Muhammad, S.; Alarfaji, S.S.; Kargar, H.; Arshad, M.U. Synthesis, crystal structure, Hirshfeld surface analysis, and computational study of a novel organic salt obtained from benzylamine and an acidic component. *ACS Omega* **2021**, 6, 22357-22366.
26. Mohamed, S.K.; Akkurt, M.; Hawaiz, F.E.; Ayoob, M.M.; Hosten, E. Crystal structure of (6E, 20E)-3,24-difluoro-13,14,28,29-tetrahydro-5H,22H-tetrabenzo[e,j,p,u][1,4,12,15] tetraoxa-cyclodocosine-5,22-dione. *Acta Cryst. E* **2017**, 73, 13-16.
27. Zhang, Y.; Pan, Y.Q.; Yu, M.; Xu, X.; Dong, W.K. Single-armed salamo-like dioxime and its multinuclear Cu(II), Zn(II) and Cd(II) complexes: Syntheses, structural characterizations, Hirshfeld analyses and fluorescence properties. *Appl. Organomet. Chem.* **2019**, 33, e5240.

28. Al-Sehemi, A.G.; Irfan, A.; Alrumman, S.A.; Hesham, A. Antibacterial activities, DFT and QSAR studies of quinazolinone compounds. *Bull. Chem. Soc. Ethiop.* **2016**, 30, 307-316.
29. Nataraj, A.; Balachandran, V.; Karthick, T. Molecular structure, vibrational spectra, first hyperpolarizability and HOMO–LUMO analysis of *p*-acetylbenzonitrile using quantum chemical calculation. *J. Mol. Struct.* **2013**, 1038, 134-144.
30. Prashanth, J.; Ramesh, G.; Naik, J.L.; Ojha, J.K.; Reddy, B.V. Molecular geometry, NBO analysis, hyperpolarizability and HOMO-LUMO energies of 2-azido-1-phenylethanone using quantum chemical calculations. *Mater. Today* **2016**, 3, 3761-3769.
31. Şahin, Z.S.; Kantar, G.K.; Şaşmaz, S.; Büyükgüngör, O. Synthesis, molecular structure, spectroscopic analysis, thermodynamic parameters and molecular modelling studies of (2-methoxyphenyl) oxalate. *J. Mol. Struct.* **2015**, 1087, 104-112.
32. Karunakaran, V.; Balachandran, V. FT-IR, FT-Raman spectra, NBO, HOMO–LUMO and thermodynamic functions of 4-chloro-3-nitrobenzaldehyde based on ab initio HF and DFT calculations. *Spectrochim. Acta A Mol. Biomol. Spectrosc.* **2012**, 98, 229-239.
33. Zinad, D.S.; Mahal, A.; Salman, G.A.; Shareef, O.A.; Pratama, M.R.F. Molecular docking and DFT study of synthesized oxazine derivatives. *Egypt. J. Chem.* **2022**, 65, 231-240.
34. Mohamad, H.A.; Ali, K.O.; Gerber, T.A.; Hosten, E.C. Novel palladium(II) complex derived from mixed ligands of dithizone and triphenylphosphine synthesis, characterization, crystal structure, and DFT study. *Bull. Chem. Soc. Ethiop.* **2022**, 36, 617-626.
35. Olalekan, T.E.; Akintemi, E.O.; Van Brecht, B.; Watkins, G.M. Synthesis, characterization and DFT studies of Schiff bases of p-methoxysalicylaldehyde. *Bull. Chem. Soc. Ethiop.* **2023**, 37, 675-688.
36. Khan, M.D.; Shakya, S.; Vu, H.H.T.; Habte, L.; Ahn, J.W. Low concentrated phosphorus sorption in aqueous medium on aragonite synthesized by carbonation of seashells: Optimization, kinetics, and mechanism study. *J. Environ. Manage.* **2021**, 280, 111652.
37. Shakya, S.; Khan, I.M.; Ahmad, M. Charge transfer complex based real-time colorimetric chemosensor for rapid recognition of dinitrobenzene and discriminative detection of Fe^{2+} ions in aqueous media and human haemoglobin. *J. Photochem. Photobiol. A* **2020**, 392, 112402.
38. Ahmed, A.; Fatima, A.; Shakya, S.; Rahman, Q.I.; Ahmad, M.; Javed, S.; AlSalem, H.S.; Ahmad, A. Crystal structure, topology, DFT and hirshfeld surface analysis of a novel charge transfer complex (L3) of anthraquinone and 4-{[(anthracen-9-yl)methyl] amino}-benzoic acid (L2) exhibiting photocatalytic properties: An experimental and theoretical approach. *Molecules* **2022**, 27, 1724.
39. Salih, R.H.H.; Hasan, A.H.; Hussein, A.J.; Samad, M.K.; Shakya, S.; Jamalis, J.; Hawaiz, F.E.; Pratama, M.R.F. One-pot synthesis, molecular docking, ADMET, and DFT studies of novel pyrazolines as promising SARS-CoV-2 main protease inhibitors. *Res. Chem. Intermed.* **2022**, 48, 4729-4751.